

# Rapid evaporation at the superheat limit

V. T. NGUYEN, R. M. FURZELAND and M. J. M. IJPELAAR

Shell Research Limited, Thornton Research Centre, P.O. Box 1, Chester CH1 3SH, U.K.

(Received 19 March 1987 and in final form 8 February 1988)

**Abstract**—A novel approach to modelling of the mass transfer flux in rapid evaporation at the superheat limit is proposed. The key concept of this approach is that, at the superheat limit, the mass transfer flux is determined by the velocity of the expanding bubble interface relative to the surrounding liquid. This is the inverse of current concepts of mass transfer during boiling. The model has been applied to the case of a butane droplet evaporating at the superheat limit. The simulation results are in general agreement with experimental measurements published in the literature. The model predicts that under certain circumstances more violent boiling can be achieved than indicated by the butane results.

## 1. INTRODUCTION

THE SUBJECT of rapid vaporization at the superheat limit has received considerable attention in the literature. It is arguably the basic phenomenon common to a number of interactions when two liquids, one at a temperature significantly above the boiling point of the second, are brought into contact. Such interactions have been encountered in a number of industries involved in metal smelting, paper making, nuclear power and liquefied natural gases [1].

Rapid vaporization occurs when a liquid becomes highly superheated. When a liquid is in contact with a solid the temperature of which is above the liquid's ambient boiling point, the degree of superheating is generally limited by the presence of nucleating sites on the surface of the solid. If, however, the hot body is liquid then the heterogeneous nucleation is suppressed and the lower boiling point liquid may attain its stability limit referred to as its superheat limit or temperature. At this value, homogeneous nucleation initiated by random density fluctuations gives rise to very rapid vaporization which is often violent.

The experimental studies to date on these interactions, which have been referred to variously as thermal explosions, vapour explosions, metal-coolant interactions or rapid phase transitions, can conveniently be divided into two types, namely those where bulk quantities (i.e. greater than a few grammes) of materials are caused to interact, and secondly those where only single droplets of liquids undergo phase transformation.

In the bulk experiments many complex processes occur in addition to vaporization of the superheated liquid. These include fluid mixing, fragmentation, transient heat transfer, and multiphase flow. It is seen therefore that, because of their complexity, the bulk experiments cannot easily be used to define the fundamental characteristics of rapid vaporization. Generally these experiments serve to give data on the initiation and propagation of the event and the resultant pressure and energy yields.

In contrast, by careful design, the small-scale experiments involving single droplets can be made free of the complexities referred to above and the basic vaporization process can be studied in detail. The single droplet approach was the subject of a recent study by Shepherd and Sturtevant [2] of rapid vaporization of butane at its superheat limit.

In this paper we propose a radically new description of rapid evaporation and formulate it in terms of a mathematical model. We apply these concepts to the behaviour of a superheated butane droplet as studied by Shepherd and Sturtevant and show that our model forms the basis for a better understanding of the large-scale interactions.

## 2. EXPERIMENTAL MEASUREMENT OF RAPID VAPORIZATION AT THE SUPERHEAT LIMIT

The experiment by Shepherd and Sturtevant follows the established bubble column technique described by Moore [3]. The technique enables a drop of liquid to be heated to its superheat limit and the resultant small-scale explosion to be observed. This is achieved by introducing a droplet of a low boiling point liquid at the base of a column of another denser immiscible liquid with a higher boiling point. An increasing temperature gradient is maintained in the upward direction in the liquid column in such a way that as the drop rises due to buoyancy effects it is simultaneously heated. It is likely that by this method the droplet is not heated uniformly and some portion of it always lags the local column temperature. The consequences of this are discussed in a later section. At a point in the column where the temperature superficially equals the superheat limit the drop undergoes spontaneous homogeneous nucleation and a violent vaporization ensues.

Shepherd and Sturtevant used butane droplets in a column of ethylene glycol in experiments in which they were able to measure the pressure pulses following the small-scale explosions of butane droplets. The

## NOMENCLATURE

$a$	parameter in spray temperature relation (equation (10))	Greek symbols	
$B$	compressibility parameter	$\alpha$	exponent for pressure ratio (equation (6))
$c_\infty$	velocity of sound in liquid remote from bubble	$\beta$	compressibility
$c_l$	liquid specific heat	$\lambda$	latent heat of vaporization
$d$	parameter in compressibility relation (equation (7))	$\rho$	density
$e$	parameter in compressibility relation (equation (7))	$\sigma$	surface tension at bubble wall
$h$	specific enthalpy	$\tau$	time integration variable
$\dot{m}$	mass flux, mass transfer rate per unit area	$\phi$	velocity potential.
$M$	mass in bubble (transferred into bubble from liquid)	Subscripts	
$n$	compressibility parameter	c	critical
$p$	pressure	l	liquid
$r$	distance from centre of bubble	R	at bubble wall
$R$	bubble radius	ref	reference value
$t$	time	s	spray
$T$	temperature	v	vapour
$T_B$	normal boiling point liquid	$\infty$	remote from bubble.
$T_{sup}$	superheat limit	Superscripts	
$u$	velocity.	0	at $t = 0$
		sat	at saturation conditions
		or "	denote first or second time derivatives.

pressure pulses triggered the flash unit used to photograph the rapidly expanding vapour bubbles. From a series of single photographs of the bubbles at various stages of expansion an overall picture of the growth process was obtained.

These results showed that:

- (1) the measured superheat limits agreed well with published data;
- (2) nucleation was always observed within the bulk material near the boundary of the droplet;
- (3) the effective velocity of the vapour-liquid interface was high initially but reached a constant value within a short time of the bubble expansion of the order of  $5 \mu\text{s}$ ;
- (4) instabilities were observed which gave rise to wrinkling of the bubble surface, the amplitude of which reached a maximum at an early stage in the bubble development and thereafter remained at this value.

From these results the authors were able to deduce that:

- (1) very high rates of mass transfer occurred from the liquid to the growing bubble which might be responsible for the observed instability and wrinkling of the evaporating surface;
- (2) the implied density of the vapour in the bubble was high;
- (3) from energy considerations, it was likely that the bubble content was not single phase but was made up of both dense vapour and liquid.

The particular experimental conditions associated with the droplet size and ethylene glycol viscosity applicable to their experiment suggested to Shepherd and Sturtevant that the mean temperature of the drop may have lagged behind that of the surrounding fluid and that the butane may not have been uniformly heated. This observation taken in conjunction with the fact that the evaporation was initiated near the droplet surface shows that the vapour bubble did not grow symmetrically in a liquid uniformly at its superheat limit. Whilst these two points do not detract from the main thrust of the conclusions by Shepherd and Sturtevant, they do give rise to complications in the modelling studies which are discussed in a later section, and also are likely to underestimate the severity of the rapid vaporization encountered in large-scale interactions.

### 3. BUBBLE GROWTH IN HIGHLY SUPERHEATED LIQUIDS

#### 3.1. Bubble interface equation of motion

Figure 1 summarizes the concepts of our idealized bubble growth and expansion model applied to highly superheated liquids. We consider a single vapour embryo which has been homogeneously nucleated in the bulk of a highly superheated liquid. The embryo is remote from any boundary surface such that for all stages of its growth, spherical symmetry can be assumed.

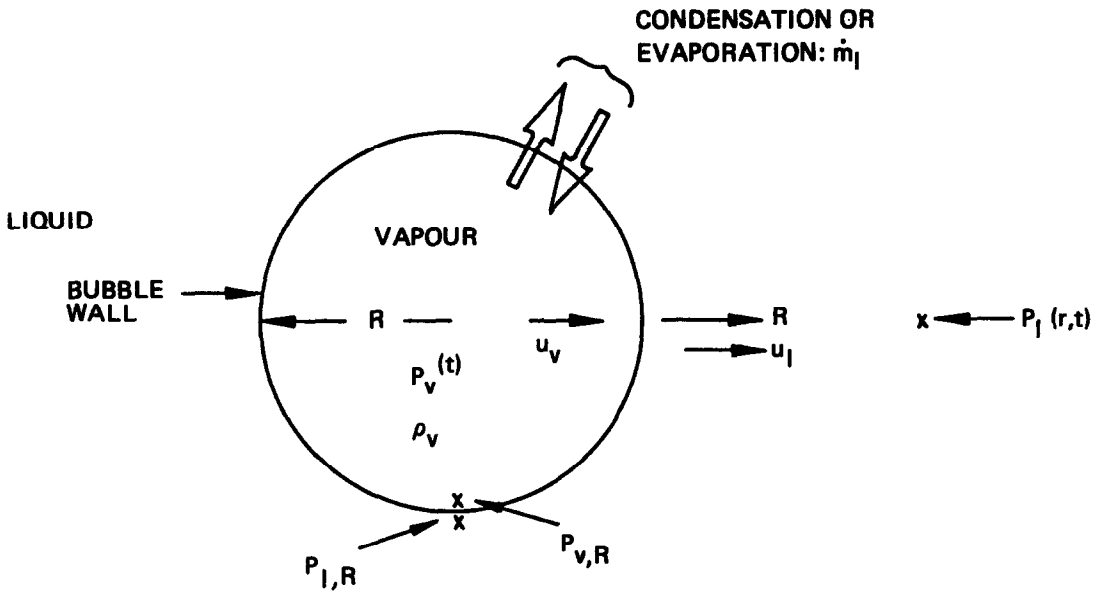


FIG. 1. Schematics of bubble growth.

A velocity potential  $\phi(r, t)$  is defined in the liquid such that the local velocity in the liquid is given by

$$u_l = \frac{\partial \phi}{\partial r}(r, t).$$

The value of  $u_l$  at the bubble interface is important in the calculations and is denoted by a second subscript 'R' thus:  $u_{l,R}$ .

Pressure in the vapour and liquid are respectively  $p_v$  and  $p_l$ . We make the assumption that  $\partial p_v / \partial r = 0$ , i.e.  $p_v$  is spatially uniform throughout the vapour; this is valid for situations where disturbances within the bubble are propagated in a time shorter than the response time of the bubble [6].

The temperature within the liquid is denoted by  $T_l$  which can be uniform, if the liquid is evenly superheated, or has a radial dependence around the bubble. Again, for ease of solution, we have restricted the temperature distribution to one dimension in spherical coordinates. The temperature within the bubble will be considered in a later section.

The bubble of radius  $R$  is subjected to an internal pressure  $p_v$ . This pressure  $p_v$  is approximately the saturated vapour pressure of the liquid at its superheat limit. It is the main cause of bubble growth and is maintained at a high value because of the surrounding liquid which is vaporized into the bubble. The problem is then one of bubble growth with vaporization at the interfacial walls, and is similar to the cavitation studied by Fujikawa and Akamatsu [4]. Following these authors, the bubble interface motion can be described by a modified Rayleigh equation which includes first-order corrections for liquid compressibility and mass transfer effects

$$\begin{aligned} & R \left( \ddot{R} - \frac{\dot{m}}{\rho_\infty} \right) \left[ 1 - \frac{1}{c_\infty} \left( 2\dot{R} - \frac{\dot{m}}{\rho_\infty} \right) \right] \\ & + \frac{3}{2} \left( \dot{R} - \frac{\dot{m}}{\rho_\infty} \right) \left[ \left( \dot{R} + \frac{1}{3} \frac{\dot{m}}{\rho_\infty} \right) - \frac{1}{c_\infty} \left( \frac{4}{3} \dot{R}^2 \right) \right] \\ & = \frac{1}{\rho_\infty} \left[ (p_{l,R} - p_\infty) + \frac{1}{c_\infty} (R \dot{p}_{l,R}) \right] \quad (1) \end{aligned}$$

where  $\dot{m}$  is the mass transfer rate per unit area,  $c_\infty$  the velocity of sound in the liquid remote from the bubble,  $\rho_\infty$  the liquid density remote from the bubble,  $p_{l,R}$  the pressure in the liquid at the bubble wall, an overdot '' indicates differentiation with respect to time,  $\dot{m}$  is  $d(\dot{m})/dt$ ,  $\dot{R}$  is  $d(\dot{R})/dt$ , and  $\dot{p}_{l,R}$  is  $d(p_l)/dt$ .

The standard Rayleigh equation is recovered from equation (1) by setting  $\dot{m} = 0$  (equilibrium vaporization/condensation) and  $c_\infty \rightarrow \infty$  (incompressible liquid).

### 3.2. Mass transfer rates in evaporation at the superheat limit

Equation (1) shows the relationship between the mass transfer flux and other bubble growth parameters. Evaporation at the superheat limit can give rise to large mass transfer fluxes ( $\dot{m}$ ) at the interface. It is seen therefore that  $\dot{m}$  has an important effect on the bubble growth process as described by equation (1). Additionally a liquid at its superheat limit is in the metastable phase, and hence the evaluation of  $\dot{m}$  is particularly complex. Recent calculations make use of kinetic theory to give evaporation fluxes dependent on the state variables  $p, T$  [4]. It can be shown, see Appendix, that such fluxes are stabilizing factors in

bubble growth in that they act to oppose the current bubble behaviour. This limitation, whilst acceptable in the case of slightly superheated and sub-cooled liquids, is not realistic at the limit of superheating. A further assumption of kinetic theory of evaporation fluxes is that the mass transferred into the bubble appears only in vapour form.

Our model is based on the premise that, because the superheat limit is an unstable region, different concepts are required to describe the process of bubble growth.

Our first postulate is that the mass transfer rate per unit area,  $\dot{m}$ , can no longer be calculated from the state variables  $p$  and  $T$ , but is rather a function of the wall and liquid velocities. At low superheats the rate of mass transfer determines the velocity of the interfacial liquid relative to the bubble wall. For the case of high superheats, however, we postulate that the relationship is reversed and that it is the mass transfer rate which is determined by the relative interfacial liquid velocity.† This leads to a definition of  $\dot{m}$  which is applicable to the case of phase change at a moving boundary. Furthermore, for reasons to be shown later, we remove the restriction that the mass transferred into the bubble is wholly vapour. We suggest that superheated liquid may be entrained into the bubble and there is partially vaporized to produce a vapour and microscopic droplets or spray. From this process we can therefore identify three terms:  $\dot{m}_l$ ,  $\dot{m}_v$  and  $\dot{m}_s$ , where  $\dot{m}_l$  is the flux of liquid entrained across the bubble boundary and may be identified with the  $\dot{m}$  of equation (1),  $\dot{m}_v$  is the flux of vapour formed and  $\dot{m}_s$  (subscript s stands for spray) is the flux of droplet formed within the bubble. By conservation of mass it is seen that

$$\dot{m}_l = \dot{m}_v + \dot{m}_s. \quad (2)$$

Having identified  $\dot{m}$  as  $\dot{m}_l$ , we assume that all three  $\dot{m}$  terms are given by the normal requirements of mass continuity at the bubble wall

$$\dot{m}_l = \rho_l(\dot{R} - u_{l,R}) \quad (3)$$

$$\dot{m}_s = \rho_s(\dot{R} - u_{s,R}) \quad (4)$$

$$\dot{m}_v = \rho_v(\dot{R} - u_{v,R}) \quad (5)$$

and the densities are defined by

$$\rho_l = \rho_l^{\text{sat}}(T_l)$$

$$\rho_s = \rho_s^{\text{sat}}(T_s)$$

$$\rho_v = \rho_v(T_v, p_v).$$

It is implied in these definitions that the most significant factor that changes the liquid densities is the temperature, and that pressure effects are only of secondary importance. This is clear when we show at a later stage the form of the liquid equation of state.

The superficial velocities of the vapour and spray at the bubble interface are  $u_{v,R}$  and  $u_{s,R}$ , respectively. We make the fundamental postulate that the interfacial liquid velocity is related to the degree of superheating, which is expressible in terms of the saturated vapour pressure. Furthermore, it can be shown from ref. [4] that this velocity should also be dependent on liquid compressibility. These factors are combined to give an equation for  $u_{l,R}$  of the form

$$u_{l,R} = \dot{R} \left[ 1 - \left( \frac{p^{\text{sat}}(T_l^0) - p_\infty}{p_c - p_\infty} \right)^\alpha \right] \quad (6)$$

where  $p^{\text{sat}}(T_l^0)$  is the saturation pressure at the initial liquid temperature,  $p_c$  the critical pressure,  $p_\infty$  the far-field ambient pressure,  $\dot{R}$  the bubble interface velocity, and  $\alpha$  a dimensionless parameter which gives the dependence of  $u_{l,R}$  on the superheated liquid compressibility.

It can be shown from the equation of state that the compressibility of the superheated liquid can be empirically expressed in terms of the compressibility at its ambient boiling point and the superheat by

$$\beta_l = \beta_b(1 + d\Delta T^e) \quad (7)$$

where  $\beta_l$  is the compressibility of superheated liquid,  $\beta_b$  the compressibility of liquid at its ambient boiling point,  $\Delta T$  the degree of superheat,  $e$  an empirically determined parameter, which is 1.523 for butane up to 80% of its maximum superheating, and  $d$  an empirically determined parameter; for butane it is  $1.945 \times 10^{-6}$ .

We make the suggestion that the dimensionless parameter  $\alpha$  be identified with the dimensionless parameter  $e$ . Thus  $\alpha$  should be determined for the appropriate liquids and conditions before equation (6) can be used.

Equation (6) gives a value of the interfacial liquid velocity which embodies our concept of phase change at large superheats where we postulate that the vapour generation rate, which in turn controls the violence of the phenomenon, is not dependent on thermal processes alone. We suggest that physically the rate at which mass is transferred across the phase boundary is dependent upon the rate at which liquid can be 'swept up' by the moving bubble wall, and that the difference between the wall and liquid velocities at the bubble boundary is a measure of the ease with which matter is transferred from the liquid to the bubble. This in turn is related to the rate of vapour production via equations (2) and (3).

At the upper limit of the critical point  $u_{l,R} = 0$ , and hence, from equation (3),  $\dot{m}_l = \rho_l \dot{R}$ . This result implies that the movement of the phase boundary at the critical point is not resisted and there is a free interchange of mass between the liquid and the bubble. In practice this is indeed the case because at the critical point the vapour and liquid phases merge and are indistinguishable. At small values of  $p^{\text{sat}}(T_l^0)$ , that is for small superheats,  $u_{l,R}$  is approximately  $\dot{R}$ . In this

† The low superheat case is analogous to diffusion controlled bubble growth. The high superheat case is analogous to the inertia controlled growth, but with the driving pressure being maintained.

case the rate of mass transfer associated with the moving boundary is seen to be small, by substitution in equation (3), as expected.

### 3.3. Momentum

At the bubble interface the following momentum equation is applicable:

$$p_{l,R} = p_{v,R} - \frac{2\sigma}{R} - [\dot{m}_v(u_{v,R} - u_{l,R}) + \dot{m}_s(u_{s,R} - u_{l,R})] \quad (8)$$

where  $\sigma$  is the surface tension.

In general the surface tension contribution becomes negligible in comparison to the other terms at any significant value of bubble radius. Equation (8) emphasizes the importance of the mass transfer terms in the momentum conservation.

### 3.4. Energy balance for vapour and spray production

The energy conservation requirement of the flashing which produces the vapour from the superheated liquid transferred across the boundary is observed in an equation of the form

$$\dot{m}_l h_l(T_1) = \dot{m}_v h_v(T_1) + \dot{m}_s h_s(T_s) \quad (9)$$

where  $h$  is the specific enthalpy of the liquid or vapour evaluated at the appropriate temperature, and in this case we considered  $T_v$  to be at  $T_1$ . Heat fluxes were not included in this energy balance for reasons to be explained below.

### 3.5. Temperature of liquid within bubble

Our definition of the mass transfer rate  $\dot{m}_l$  reflects the view that bubble growth in highly superheated liquids is such a violent process that the mechanical constraints dominate any thermal transfer process. However, when we examine the enthalpy content of the superheated liquid we find that the superheat enthalpy is not sufficient to convert all the liquid into vapour. We need to establish the proportion of  $\dot{m}_v$  to  $\dot{m}_s$  defined in equation (2). We approach this through consideration of the temperatures of the different components.

We consider that  $\dot{m}_l$  is produced at the local liquid temperature  $T_l$ ,  $\dot{m}_v$  is formed from  $\dot{m}_l$  also at temperature  $T_l$ , whereas  $\dot{m}_s$  is produced at a spray temperature  $T_s$ . If we consider the incoming liquid which is at  $T_l$ , flashing into vapour which is also at  $T_l$ , it is clear that the latent heat of vaporization must come from cooling of the liquid that has not vaporized (i.e. the spray). Of necessity therefore,  $T_s$  is less than  $T_l$ . The following relation has been chosen to describe  $T_s$ :

$$T_s = T_B + a(T_l - T_B) \quad (10)$$

where  $T_B$  is the normal boiling point of the liquid and  $a$  an adjustable parameter which by manipulation of equations (9) and (10), with suitable approximation, can be expressed in terms of a Jakob like number

$$a = 1 - \frac{\dot{m}_v \lambda}{\dot{m}_s c_l (T_l - T_B)} \quad (11)$$

where  $c_l$  is the liquid specific heat and  $\lambda$  the latent heat of vaporization.

Alternatively, following Hahne and Grigull [7]  $a$  can be identified with a temperature profile parameter in the two-phase boundary layer. Figure 2 shows the temperature profile in the two-phase region close to a heated wall in contact with boiling liquid. There is a significant change of slope at around 0.6 of the boundary layer thickness. We suggest that the temperature in the region behind the expanding bubble interface follows a similar pattern to that shown in Fig. 2. The appropriate value for  $a$  is therefore 0.4.

### 3.6. Temperature distributions

The evidence from experiments such as those by Shepherd and Sturtevant shows that the vaporization time for millimetre size butane droplets is of the order of  $10^{-5}$  s. The liquid thermal diffusivity,  $k_l$ , for butane at these temperatures is of the order of  $10^{-7}$  m<sup>2</sup> s<sup>-1</sup>. It is seen therefore that for the characteristic event times, the diffusion length,  $\sqrt{(k_l t)}$ , for the thermal front is less than the depth of liquid around the bubble that has been transferred across the phase boundary. This leads us to postulate that heat transfer in the liquid is not a significant factor and to conclude that any temperature profile that may exist in the liquid remains unchanged over the time scale of interest.

The temperature distribution within the bubble is a more complex problem. We have shown earlier that from energy conservation both vapour and droplets are formed at different temperatures within the bubble. We restrict the interaction between the vapour and spray within the bubble so that there can be no mass transfer between the two, although thermal exchanges may take place. That is, once formed the mass of each component phase in the bubble is conserved but heat can flow from one phase to the other. This leads to the result that the components of the bubble content can be at different temperatures,  $T_v$  for the vapour and  $T_s$  for the spray. We further simplify the problem by considering that the temperatures inside the bubble are spatially invariant but can change with time, that is

$$\frac{\partial T}{\partial r} = 0, \quad \frac{\partial T}{\partial t} \neq 0.$$

### 3.7. Global mass and energy conservation

The mass conservation of the two components in the bubble can be expressed in terms of a volume relationship

$$\frac{M_v}{\rho_v} + \frac{M_s}{\rho_s} = \frac{4}{3} \pi R^3 \quad (12)$$

where  $\rho_v$  is the vapour density within the bubble

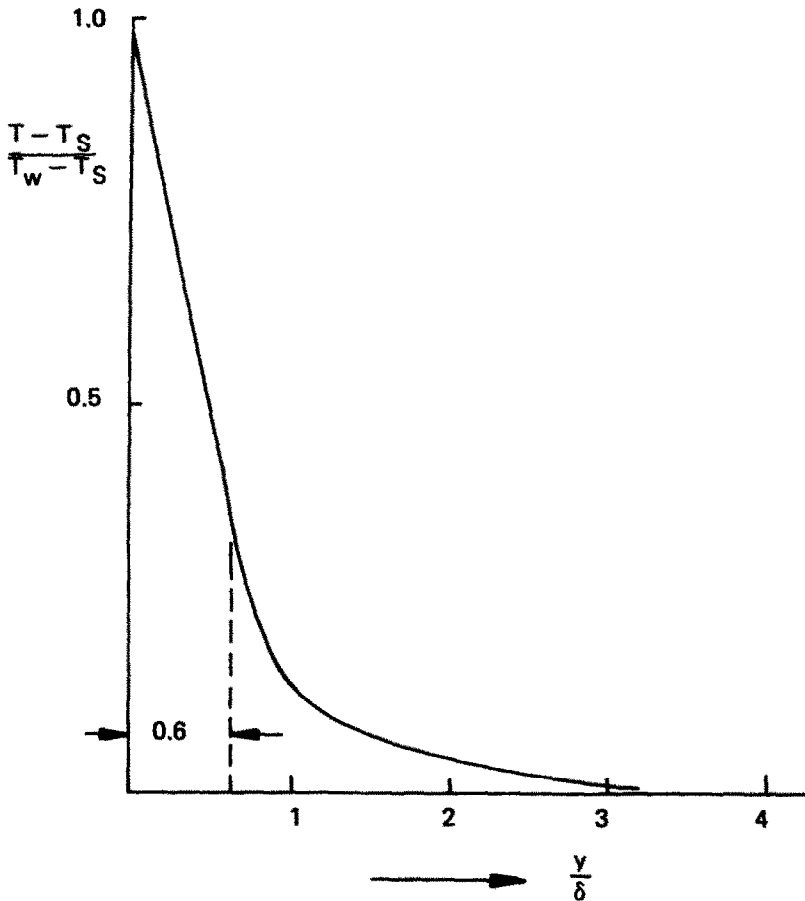


FIG. 2. Temperature profile in superheated boundary layer close to a hot surface in contact with boiling liquid (taken from ref. [7]):  $\delta$  is the boundary layer thickness;  $T_w$  the wall temperature and  $T_s$  the liquid saturation temperature.

and satisfies the Redlich-Kwong equation of state with  $p_v, T_v$ .

The energy conservation for the system gives rise to an equation of the form

$$4\pi R^2 \dot{m}_1 h_1(T_1) = \frac{d}{dt}(M_v h_v(T_v)) + \frac{d}{dt}(M_s h_s(T_s)) + (p_v - p_\infty) \frac{d}{dt} \left( \frac{M_v}{\rho_v} \right) \quad (13)$$

where  $M_v$  and  $M_s$  are the total masses of vapour and spray in the bubble and  $p_\infty$  is the ambient pressure.

This equation shows that the energy source is the superheated liquid. This energy is transferred into the bubble content but a part of it is accounted for by the expansion work done by the bubble against the surroundings.

3.8. Far-field pressure

Finally, in the experiments by Shepherd and Sturtevant the pressure field in the liquid remote from the bubble was measured. In our model we follow the procedure given in ref. [4] and obtain the far-field

pressure from perturbation theory with first-order corrections for liquid compressibility and mass transfer effects

$$p_l(r, t) = -B + (p_\infty + B) \left\{ 1 - \frac{(n-1)}{c_\infty^2} \times \left[ \frac{\partial \phi(r, \eta)}{\partial t} + \frac{1}{2} \left( \frac{\partial \phi(r, \eta)}{\partial r} \right)^2 \right]^{n/(n-1)} \right\} \quad (14)$$

where

$$\phi(r, \eta) = -\frac{R^2}{r} \left\{ \dot{R} - \frac{\dot{m}_1}{\rho_\infty} - \frac{1}{c_\infty} \left[ 2\dot{R} \left( \dot{R} - \frac{\dot{m}_1}{\rho_\infty} \right) + R \left( \dot{R} - \frac{\dot{m}_1}{\rho_\infty} \right) \right] \right\} \quad (15)$$

$r$  is the distance to the centre of the bubble,  $\phi$  the velocity potential,  $\eta$  the initial time of the outgoing pressure, and is related to the current time  $t$  by the equation

$$t = \eta + \frac{r - R(\eta)}{c_\infty} \quad (16)$$

$B$  and  $n$  are constants used in the liquid equation of state of the form

$$\left(\frac{\rho}{\rho_{\text{ref}}}\right)^n = \frac{p+B}{p_{\text{ref}}+B} \quad (17)$$

Values of  $B$  and  $n$  can be calculated from published liquid density data.

#### 4. ADAPTATION OF MODEL TO REFLECT CONDITIONS OF EXPERIMENT BY SHEPHERD AND STURTEVANT

In order to apply the set of equations derived in the previous section to the results obtained by Shepherd and Sturtevant, we shall consider in turn a number of points raised by the authors about their experiment.

It was stated that the heating of the butane droplets was not ideal by virtue of both the size of the droplets and the viscosity changes in the heating fluid. The values of droplet size in these experiments can be compared with the smaller ones used by Porteous and Blander [5] which should in principle yield better heating characteristics. The result of the non-ideal heating is that the temperature within the droplet is likely to lag behind that of the column, thus only a thin layer of the liquid is heated to the superheat limit temperature, and the bulk of the droplet remains at lower temperatures. This does not contradict the observation that the rapid evaporation occurred at temperatures similar to those reported in earlier work because the initiating event within the droplet must occur in the fully superheated layer. This indeed is confirmed by another observation in the experiment that nucleation sites always occurred within the droplets but rather close to their surfaces. The temperature profile within the droplet would have had a major effect on the subsequent evaporation.

Firstly, although the evaporation and bubble growth may have been violent at the initial stage when the liquid is at its superheat limit, this violence could not be maintained in the time of interest. This is evident if we consider that the driving pressure for growth is the saturated vapour pressure, and in the case of a decreasing temperature the saturated vapour pressure must also decrease. We believe that the data on the bubble growth support this view even though they do not refer to a single droplet. It is seen from these data that the growth rate, or bubble wall velocity, was of the order of  $14 \text{ m s}^{-1}$  for times greater than  $10 \mu\text{s}$ . Assuming that the bubble growth is essentially inertia controlled this wall velocity is commensurate with a pressure differential between the bubble and infinity of the order of 2 bar and not 17 bar as would be the case if the butane were at the superheat limit.

Secondly, because the nucleation sites occurred

close to the droplet surfaces, the proportion of the total bubble area from which evaporation occurred is strongly time dependent. This is because only the butane evaporated and the ethylene glycol has made no contribution to the bubble growth.

We have accounted for the above two factors in our calculations by ascribing a temperature profile to the butane and applying a correction factor to the evaporation area. This last factor was achieved by considering that the evaporation only occurred from a fraction of the total bubble area. This fraction was a geometrical function of the bubble radius.

A further difficulty arose with regard to the computation of the pressure pulse. The distance from the droplet to the pressure transducer was not clearly defined by Shepherd and Sturtevant. We have assumed in our calculations that the transducer was 25 mm from the signal source. We have not taken into account the acoustic properties of the ethylene glycol in our calculations, but we estimate that these would only affect the shape of the far-field pressure pulse and not the essential dynamics of the bubble itself.

The reverberation behaviour of the butane droplet postulated by Shepherd and Sturtevant is very plausible but difficult to model. Equally the interference between various types of reflections at the transducer is difficult to estimate without full details of the experimental apparatus. For these reasons our pressure pulse data are only idealized free field values and can be expected to agree qualitatively with experiments.

#### 5. COMPARISON OF NUMERICAL RESULTS WITH EXPERIMENTAL VALUES

Equations (1)–(13) comprise our bubble growth model together with the Redlich–Kwong equation of state for the vapour, a specified temperature distribution in the liquid and a number of time integral and time derivative relations, namely

$$\begin{aligned} \dot{R} &= \int_0^t \dot{R} \, d\tau, & R &= \int_0^t \dot{R} \, d\tau \\ M_v &= \int_0^t 4\pi R^2 \dot{m}_v \, d\tau + M_v^0, & M_s &= \int_0^t 4\pi R^2 \dot{m}_s \, d\tau \\ \dot{m}_i &= \frac{d}{dt} \dot{m}_i, & \dot{p}_{i,R} &= \frac{d}{dt} p_{i,R}. \end{aligned}$$

These equations have been discretized implicitly in time resulting in a system of non-linear equations. This system is solved over a non-uniform time grid, which has a fine mesh spacing in the first few microseconds of the event. To aid the convergence of the numerical solution process the model variables have been transformed into dimensionless quantities similar to the nondimensionalization carried out by Florschuetz and Chao [6]. The numerical method used to solve the non-linear system is a Newton-like method with automatic structural and sensitivity

Table 1. Butane data and model parameters

Properties and parameters	Symbol	Value	Units
Conditions remote from bubble:			
liquid pressure	$p_\infty$	$1.01325 \times 10^5$	$\text{N m}^{-2}$
liquid density	$\rho_\infty$	610	$\text{kg m}^{-3}$
velocity of sound in liquid	$c_\infty$	410	$\text{m s}^{-1}$
Superheat limit	$T_{\text{sup}}$	378	K
Normal boiling point	$T_B$	272.7	K
Critical temperature	$T_c$	425	K
Critical pressure	$p_c$	$38.0 \times 10^5$	$\text{N m}^{-2}$
Surface tension at bubble wall	$\sigma$	$7.845 \times 10^{-3}$	$\text{N m}^{-1}$
Compressibility parameter†	$B$	$201.7 \times 10^5$	$\text{N m}^{-2}$
Compressibility parameter†	$n$	5	—
Spray temperature parameter	$a$	0.4	—
Liquid velocity parameter	$\alpha$	1.5	—
Reference density	$\rho_{\text{ref}}$	610	$\text{kg m}^{-3}$
Reference pressure	$p_{\text{ref}}$	$1.01325 \times 10^5$	$\text{N m}^{-2}$

† The compressibility parameters were derived from density–pressure data for butane [10].

analysis facilities, which ensures that the problem is well conditioned over the whole time grid.

Equation (14) for the liquid pressure remote from the bubble is solved separately, once the relevant values for the bubble variables in time have been calculated.

The properties of butane and other data used in our calculations are given in Table 1. The initial bubble radius and droplet radius are 0.05 and 0.5 mm, respectively. At time  $t = 0$  the system is considered to be in equilibrium at the superheat limit of butane ( $105^\circ\text{C}$ ); the set of initial conditions is then given in Table 2. The temperature profile in the liquid is such, that at the initial bubble wall the liquid is at the superheat limit and decreases radially to  $50^\circ\text{C}$  of superheat over a distance of 0.45 mm in a manner compatible with conductive heat transfer calculations.

Figures 3–7 show the comparison between our calculated results and the experimental values of Shepherd and Sturtevant. As suggested by these authors, it is likely that some features in the pressure measurements at times later than  $30 \mu\text{s}$  are not directly caused by violent evaporation but may be associated with multiple reflections in their system. Accordingly we limit our calculations to the first  $30 \mu\text{s}$  of the

process in order that comparison can be made between the model behaviour and what may be considered as data free from interference by the apparatus.

In Fig. 3 we compare the calculated bubble radii with the experimental measurements by Shepherd and Sturtevant. Calculated bubble interface velocities are compared with experimental values inferred from bubble radii in Fig. 4. It is seen that the calculated velocities are greater than the experimental ones over the time range of interest. The experimental interface velocities also appear to attain an equilibrium value very quickly after the commencement of bubble growth. This indicates that although an attempt was made in the calculations to approximate the experimental conditions of bubble growth, the simulation was still more violent than appropriate for the measurement of Shepherd and Sturtevant. Further refined calculations and comparisons with experimental velocities would have to await the availability of reliable measurements of the liquid temperature distribution in the evaporating droplet.

The mass flux  $\dot{m}_1$  as a function of time is compared in Fig. 5. The differences between computed and experimental values can be partially explained by Shepherd and Sturtevant who suggest that their method for deducing mass flux data from measurements may underestimate values for early times. The total mass  $M_1$  of liquid transferred into the bubble is not actually given in ref. [2], but can be calculated from the pressure pulse data. In Fig. 5 we compare our calculated  $M_1$  with those we derived from the published experimental measurements. We include in the theoretical values of  $M_1$  the effects of reduced evaporation area referred to previously. The value of  $M_1$  from our model calculation deviates only after  $20 \mu\text{s}$ ; it is plausible that our area correction factor underestimates the effective area at later times, and hence our data show a turn down in  $M_1$  values at large times.

The pressure pulses at a distance of 25 mm from

Table 2. Initial condition for the bubble growth model

Variable	Value at $t = 0$	Units
$R$	$0.5 \times 10^{-4}$	m
$T_v$ (superheat limit)	378	K
$\rho_v$	43.95	$\text{kg m}^{-3}$
$p_v = p_v^{\text{sat}}$ at $T_v$	$1.71 \times 10^6$	$\text{N m}^{-2}$
$T_l$ (superheat limit)	378	K
$\rho_l = \rho_\infty$	610	$\text{kg m}^{-3}$
$p_l = p_v - 2\sigma/R$	$1.71 \times 10^6$	$\text{N m}^{-2}$
$M_v = \frac{4}{3}\pi R^3 \rho_v$	$2.3 \times 10^{-11}$	kg
$M_l, M_1$	0	kg
$u_1, u_v$	0	$\text{m s}^{-1}$
All first and second time derivatives	0	



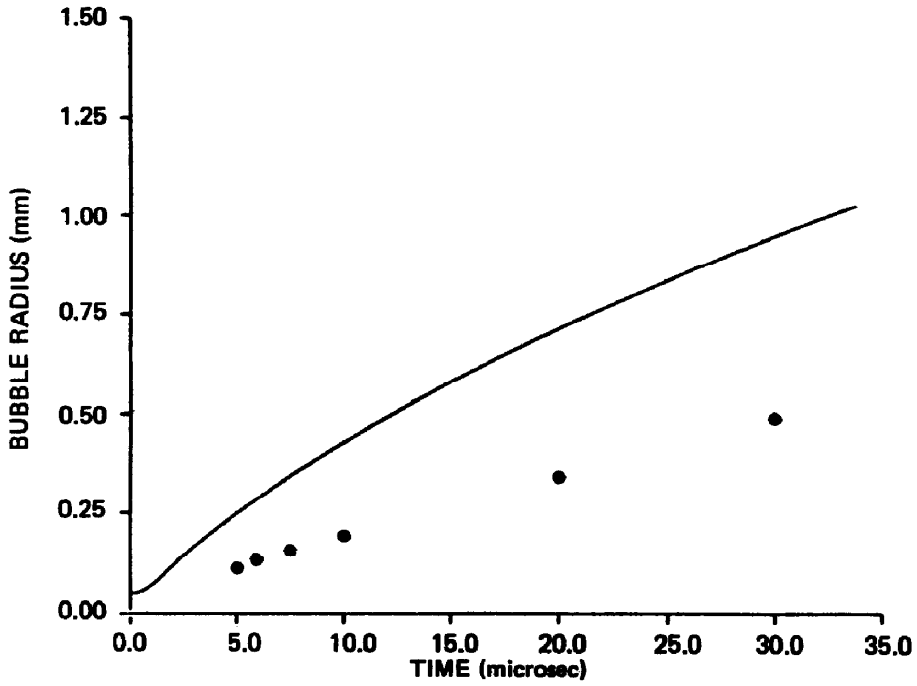


FIG. 3. Bubble growth in a superheated butane drop; —, model calculations; ●, experiment by Shepherd and Sturtevant.

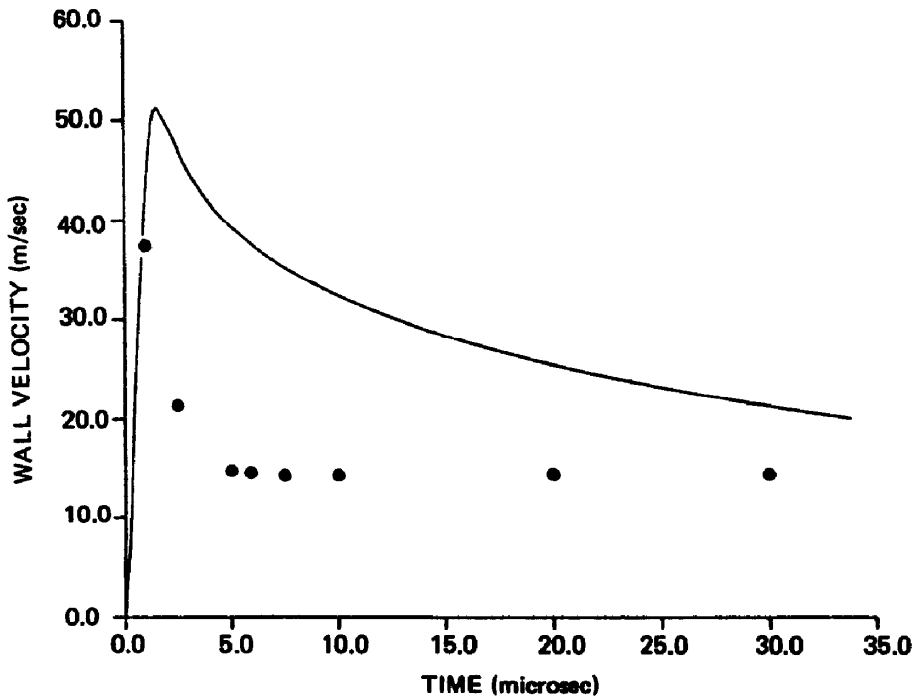


FIG. 4. Bubble wall velocity  $\dot{R}$ : —, model calculations; ●, experiment by Shepherd and Sturtevant.

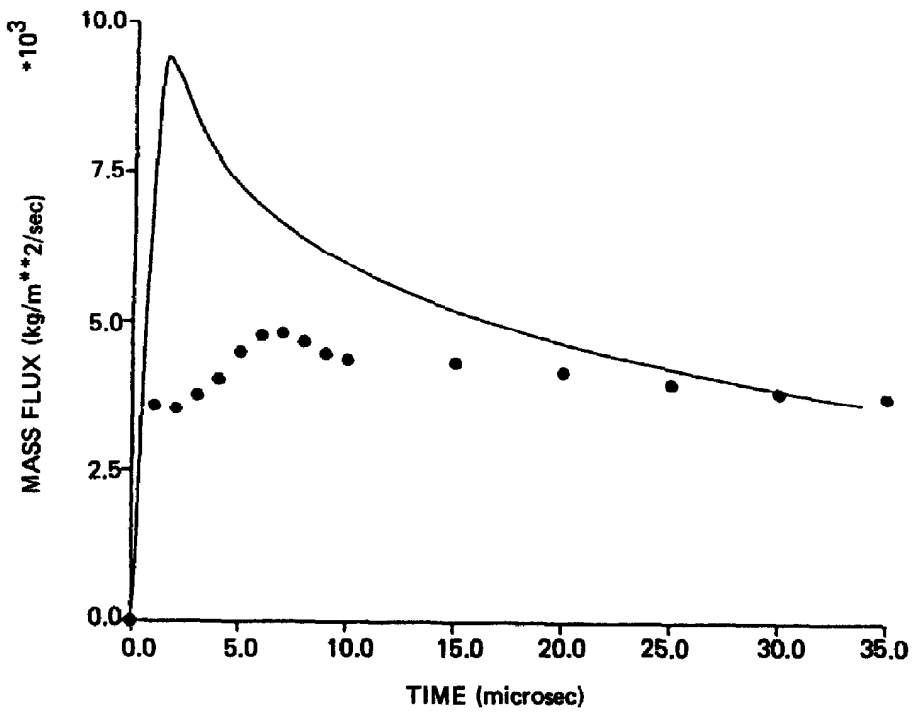


FIG. 5. Liquid to bubble mass flux  $\dot{m}_l$ : —, model calculations; ●, experiment by Shepherd and Sturtevant.

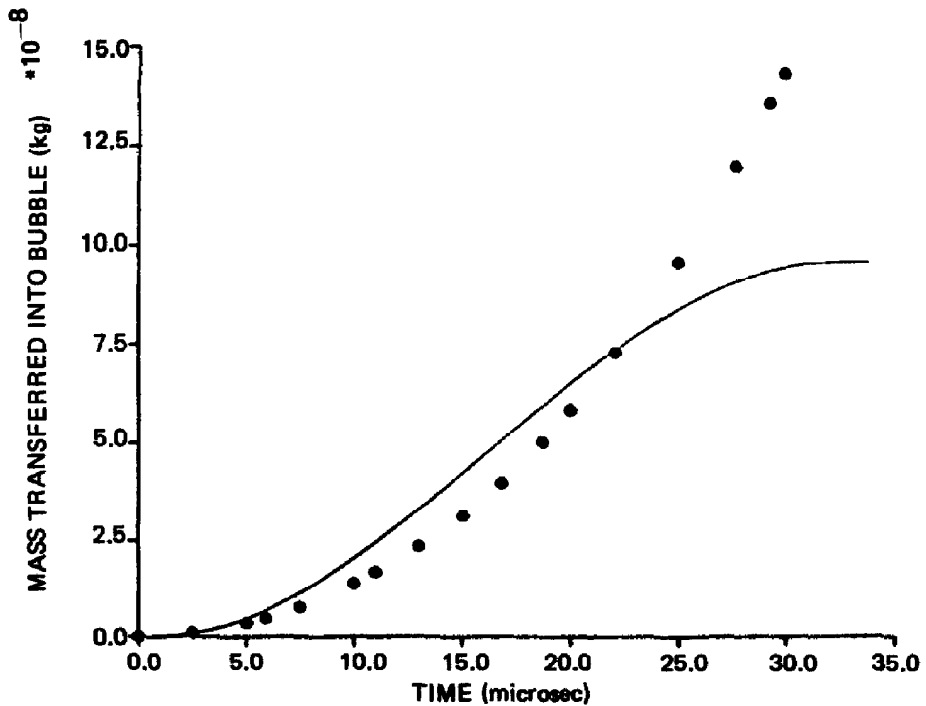


FIG. 6. Total mass of liquid transferred into the bubble  $M_l$ : —, model calculations; ●, experiment by Shepherd and Sturtevant.

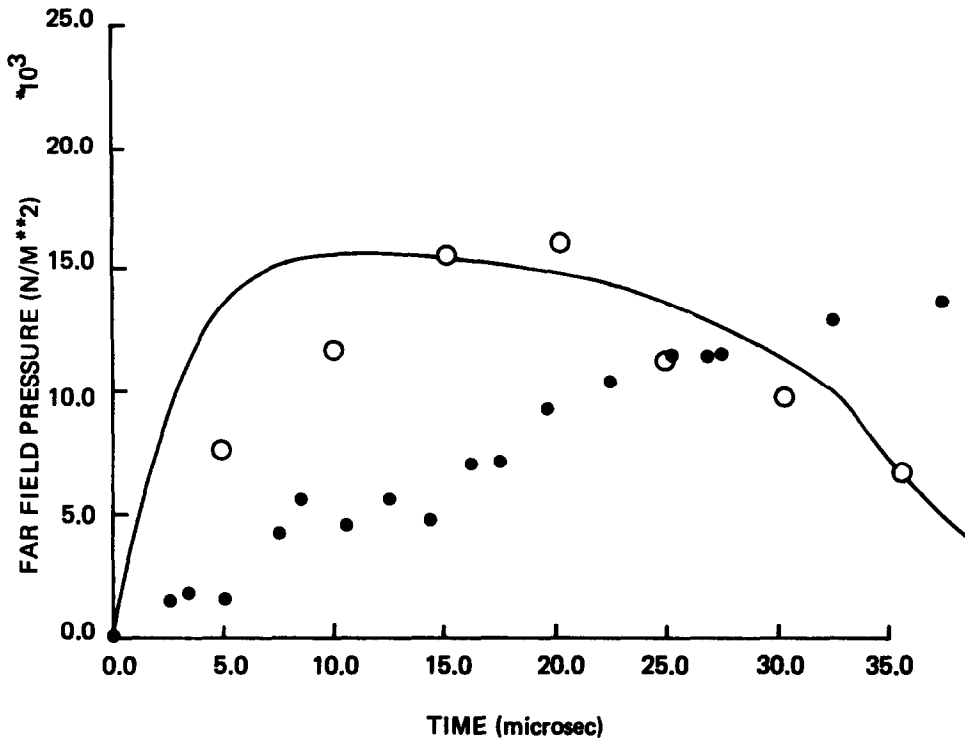


FIG. 7. Pressure in the liquid at a distance of 25 mm from the bubble centre; time axis gives microseconds after first pressure signal calculated/measured at 25 mm: —, model calculations; ●, experiments by Shepherd and Sturtevant; ○, normalized experimental data from Shepherd and Sturtevant.

the centre of the bubble are compared in Fig. 7. As discussed earlier our pressure pulse data are idealized free field values and our model does not incorporate reverberation and reflection effects. It is to be noted that the values at the time axis have been corrected for the transit time of the pulse to the point of measurement; the calculated data have been superimposed on the experimental value, such that the two initial points coincide.

It can be expected that because the model bubble growth is more violent than the experiments, the calculated and measured pressure profiles would exhibit significant differences. This is indeed the case as shown in Fig. 7. In order to establish a more realistic comparability, we also show in Fig. 7 a *normalized* pressure pulse from ref. [2]. This normalization was achieved by first of all scaling down the experimental pressures by the factor 1.83 to account for the reflected wave at the transducer [2]. The time axis for the experimental pulse was then compressed so that the pressure at a time value of 35  $\mu$ s is around 40% of its peak value as is the case for the calculated pulse. This analysis shows a closer comparability between the two pulses and qualitatively similar profiles are obtained.

## 6. DISCUSSION OF MODEL

The modelling of the rapid evaporation of metastably superheated liquid is very complex and an

empirical approach is not reliable because of the lack of well controlled and instrumented experiments. We have adopted the view that a sensible way ahead is to build up a simple model based on a number of postulates. The model can be directly compared with small-scale experiments as in the previous section and also used to predict the behaviour of less directly comparable experiments.

We highlight and discuss in this section some of these physical postulates and indicate how the model can be applied in other less directly comparable experiments.

A fundamental postulate of the present model is incorporated in equation (6). Whilst the concept is, to our knowledge, novel, we have tried to establish its relationship with more classical concepts such as liquid compressibility.

A second postulate is made in equation (10). We suggest that the results of ref. [7] can be interpreted in our model to mean that, if  $a$  is identified with the temperature profile parameter in the two-phase boundary layer, then the superheated liquid which is pulled away from the continuous liquid phase can be thought of as undergoing phase change over a distance  $0.6\delta$ , where  $\delta$  is the boundary layer thickness. Beyond  $0.6\delta$  no further phase change occurs and any remaining liquid becomes 'spray'.

The ambient pressure is taken into consideration in a number of equations in the current model. First

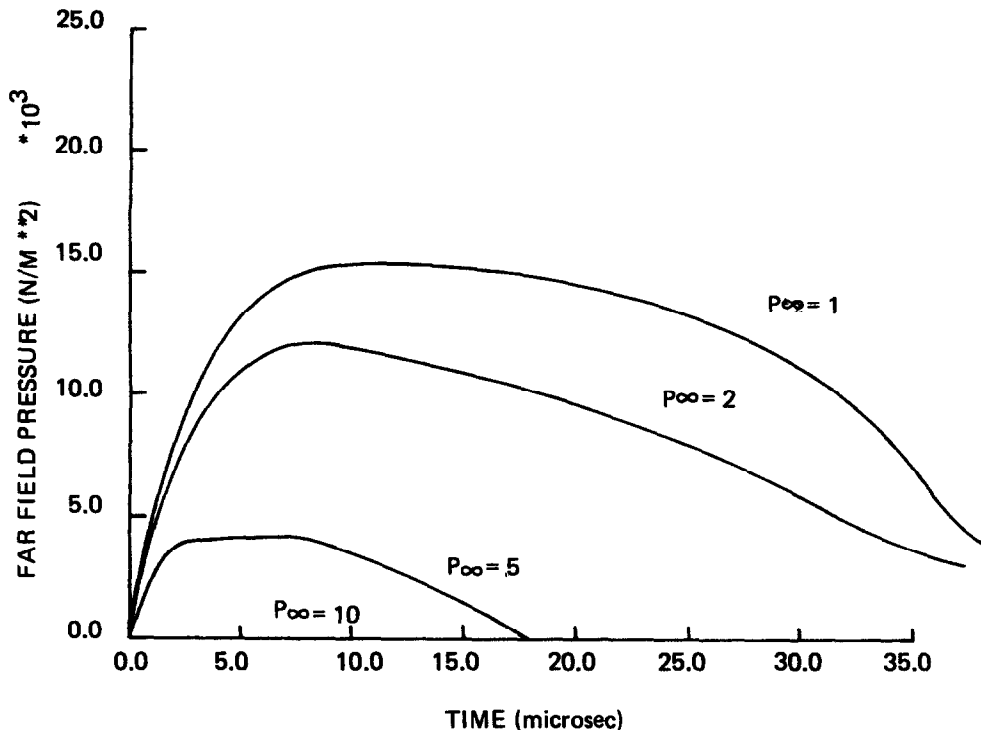


FIG. 8. Effect of rise of ambient pressure on pressure pulse in the liquid at a distance of 25 mm from bubble centre; time axis gives microseconds after first pressure signal calculated at 25 mm. Model calculations at ambient pressures of 1, 2, 5, 10 bar.

of all, it has an effect on the mass transfer relation (equation (6)), and then via this mass transfer term it affects the pressure in the liquid (equation (8)) and again it affects directly the bubble dynamics (equation (1)). Intuitively it is expected that a rise in the ambient pressure for a given superheat should lead to a slow down of the bubble growth and reduction in the far-field pressure pulse. In Fig. 8 we show the effect of increasing ambient pressure on the butane bubble under consideration. It is clear that when the ambient pressure rises to between 5 and 10 bar, the far-field pressure drops to insignificant levels. The exact transition point between violent and gentle evaporation is not readily determined because of the lack of a clear criterion. These results are in qualitative agreement with the experiments by Avedisian [8] who observed that explosive boiling of n-octane droplets disappeared around an ambient pressure of 7 bar.

Frost and Sturtevant [9] have extended the study by Shepherd and Sturtevant [2] to include the roles of ambient pressure in suppressing explosive boiling. Although their results are not in a form to be directly comparable with our calculations they reported that increasing ambient pressure reduced the violence of the rapid evaporation and that the onset of violent evaporation and nucleation of the initial microscopic bubble are not coincident. The delay is a function of the ambient pressure.

These conclusions are not at variance with the cur-

rently postulated model. The effect of pressure has already been discussed. As to the suggested delay to instability and violent evaporation, the current model only addresses the bubble growth once violent evaporation, has started. It does not deal with nucleation of the initial microscopic bubble.

## 7. CONCLUSIONS

We have proposed in our model a radical new approach to modelling of the evaporation and bubble growth in a liquid at its superheat limit. By plausible arguments we suggest that the velocity of the bubble wall determines the degree of mass transfer from what might be called the connected liquid to the two-phase bubble interior. Furthermore, we propose that this mass transfer removes liquid at the bubble surface at such a rate that thermal diffusion in the liquid around the bubble is not significant. This has the effect that the energy balance condition at the interface is simplified to an enthalpy flow balance of liquid, vapour and spray components, and any temperature profile that may exist in the liquid remains unchanged over the time scale of the bubble growth.

We have compared our model predictions with experimentally determined values of bubble growth as measured in an experiment involving a single droplet of butane. The particular conditions of the experiment were not well documented apart from a state-

ment to the effect that the liquid droplet was not uniformly superheated to its stability limit. In order to account for this factor we have introduced supplementary conditions in our calculations that essentially reduce the severity of the rapid evaporation. We stress however that these conditions may not fully reflect the true local conditions of the experiment. With these constraints the agreement between theory and experiment is reasonable. There is however the possibility that in other large-scale interactions the degree of superheating of the vaporizable liquid is greater than that achieved in ref. [2]. In these circumstances our model would predict a far more violent interaction which might be more representative of experiments involving liquid metals and water.

The effect of increasing ambient pressure is correctly predicted by the present model.

## REFERENCES

1. R. C. Reid, Rapid phase transformations, MIT-GRI, LNG Safety and Research Workshop, Vol. 1, GRI 82/0019.1 (1982).
2. J. E. Shepherd and B. Sturtevant, Rapid evaporation at the superheat limit, *J. Fluid Mech.* **121**, 379 (1982).
3. G. R. Moore, Vaporization of superheated drops in liquids, *A.I.Ch.E. J.* **19**, 909 (1959).
4. S. Fujikawa and T. Akamatsu, Effects of the non-equilibrium condensation of vapour on the pressure produced by the collapse of a bubble in a liquid, *J. Fluid Mech.* **97**, 481 (1980).
5. W. Porteous and M. Blander, Limits of superheat and explosive boiling of light hydrocarbons, halocarbons, and hydrocarbon mixtures, *A.I.Ch.E. J.* **21**, 560 (1975).
6. L. W. Florschuetz and B. T. Chao, On the mechanics of vapour bubble collapse, *Trans. ASME J. Heat Transfer* **87**, 209-220 (1965).
7. E. Hahne and U. Grigull, *Heat Transfer in Boiling*. Academic Press, New York (1977).
8. C. T. Avedisian, Effect of pressure on bubble growth within liquid droplets at the superheat limit, *Trans. ASME J. Heat Transfer* **104**, 750-757 (1982).
9. D. Frost and B. Sturtevant, Effects of ambient pressure on the stability of a liquid boiling explosively at the superheat limit, *Trans. ASME J. Heat Transfer* **108**, 418-424 (1986).
10. K. E. Starling, *Fluid Thermodynamic Properties for Light Petroleum System*. Gulf, Houston, Texas (1973).
11. J. G. Collier, *Convective Boiling and Condensation*. McGraw-Hill, New York (1972).

## APPENDIX

The evaporation/condensation flux from a liquid surface at temperature  $T_1$  into a vapour space at pressure  $p_v$  and temperature  $T_v$  is given by [11]

$$\dot{m} = A \left( \sqrt{\left(\frac{p_v^*}{T_1}\right)} - \sqrt{\left(\frac{p_v}{T_v}\right)} \right) \quad (\text{A1})$$

where  $A$  is a constant and  $p_v^*$  the saturated pressure at temperature  $T_1$ .

For bubble growth to occur  $p_v$  must be greater than the ambient pressure. In the case of a slightly superheated liquid  $p_v^*$  will be smaller than  $p_v$  whilst  $T_1$  and  $T_v$  are of the same order of magnitude. Application of equation (A1) leads to the result that  $\dot{m}$  is negative. That is, if there is a significant pressure to cause bubble growth, the same pressure will also drive a condensation flux, which in turn tends to reduce  $p_v$ , leading to a slow down of the expansion rate.

Conversely if  $p_v$  is less than  $p_v^*$  (bubble collapse) there is produced an evaporation flux which tends to reduce the collapse rate.

It is seen from the above argument that equation (A1) gives rise to evaporation/condensation fluxes that are stabilizing factors in bubble growth or collapse.

## EVAPORATION RAPIDE A LA LIMITE DE SURCHAUFFE

**Résumé**—On propose une nouvelle approche pour modéliser le flux de masse transféré en évaporation rapide à la limite de surchauffe. Le concept-clé de cette approche est qu'à la limite de surchauffe, le flux de masse transféré est déterminé par la vitesse d'expansion de l'interface de la bulle par rapport au liquide ambiant. Ceci est l'inverse des concepts courants du transfert de masse pendant l'ébullition. Le modèle est appliqué au cas d'une goutte de butane s'évaporant à la limite de surchauffe. Les résultats de la simulation sont en accord général avec les mesures expérimentales déjà publiées. Le modèle prédit que dans certaines circonstances une ébullition peut être atteinte de façon plus violente qu'indiquée par les résultats sur le butane.

## SCHNELLE VERDAMPFUNG AN DER ÜBERHITZUNGSGRENZE

**Zusammenfassung**—Es wird ein neues Modell zur Beschreibung des Stofftransports bei der schnellen Verdampfung an der Überhitzungsgrenze vorgeschlagen. Die Grundidee dieses Näherungsmodells ist, daß an der Überhitzungsgrenze der Stofftransport durch die Geschwindigkeit der expandierenden Grenzfläche einer Blase relativ zur umgebenden Flüssigkeit bestimmt ist. Dies steht im Gegensatz zu den bekannten Modellen der Stoffübertragung bei Verdampfung. Das Modell wurde auf den Fall verdampfender Butan-Tropfen an der Überhitzungsgrenze angewandt. Die Simulationsergebnisse stimmen mit experimentellen Daten aus der Literatur generell überein. Aus dem Modell ergibt sich, daß unter bestimmten Bedingungen eine bessere Verdampfung erreicht werden kann, als die Meßergebnisse von Butan aufweisen.

**БЫСТРОЕ ИСПАРЕНИЕ ПРИ ПЕРЕГРЕВЕ**

**Аннотация**—Предлагается новый подход к моделированию массопередачи при перегреве. Основная идея метода заключается в том, что при перегреве перенос массы определяется скоростью роста пузырька, что противоречит современным представлениям о переносе массы при кипении. Модель использовалась для расчета испарения капли бутана при перегреве. Результаты модельных расчетов хорошо согласуются с опубликованными экспериментальными данными. Расчеты показывают, что при определенных условиях может происходить более интенсивное кипение, чем это следует из результатов, полученных для бутана.